Polymer Chemistry

CuAAC-methacrylate interpenetrating polymer network (IPN) properties modulated by visible-light photoinitiation

Journal:	*Polymer Chemistry*
Manuscript ID	PY-ART-05-2023-000507.R1
Article Type:	Paper
Date Submitted by the Author:	29-Jun-2023
Complete List of Authors:	Kabra, Mukund; University of Delaware, Department of Chemical and Biomolecular Engineering Kloxin, Christoper; University of Delaware, Materials Science and Engineering; University of Delaware, Chemical and Biomolecular Engineering

ARTICLE

CuAAC-methacrylate interpenetrating polymer network (IPN) properties modulated by visible-light photoinitiation

Mukund Kabra,*[a] Christopher J. Kloxin [a,b]

Received 00th January 20xx,
Accepted 00th January 20xx

DOI: 10.1039/x0xx00000x

Interpenetrating polymer networks (IPNs) are a class of materials with interwoven polymers that exhibit unique blended or enhanced properties useful to a variety of applications, ranging from restorative protective materials to conductive membranes and hydrophobic adhesives. The IPN formation kinetics can play a critical role in the development of the underlying morphology and in turn the properties of the material. Dual photoinitiation of copper-catalyzed azide–alkyne (CuAAC) and radical mediated methacrylate polymerization chemistries enable the manipulation of IPN microstructure and properties by controlling the kinetics of IPN formation via the intensity of the initiating light. Specifically, azide and alkyne-based polyethylene glycol monomers and tetraethylene glycol dimethacrylate (TEGDMA) were polymerized in a single pot to form IPNs and the properties were evaluated as a function of the photoinitiating light intensity. Morphological differences as a function of intensity were observed in the IPNs as determined by thermomechanical properties and phase-contrast imaging in tapping mode atomic force microscopy (AFM). At moderate intensities (20 mW/cm^2) of visible light (470 nm), the TEGDMA polymerization gels first and therefore forms the underlying network scaffold. At low intensities (0.2 mW/cm^2), the CuAAC polymerization can gel first. The ability to switch sequence of gelation and IPN trajectory (simultaneous vs. sequential), affords control over phase separation behavior. Thus, light not only allows for spatial and temporal control over the IPN formation but also provides control over their thermomechanical properties, representing a route for facile IPNs design, synthesis, and application.

Introduction

Covalently crosslinked polymer networks are used in a variety of advanced materials applications since they are lightweight and chemically robust. Their mechanical properties are readily tuned through monomer selection, leading to materials with enhanced mechanical strength, vibration damping, ionic conductivity, thermal insulation, hydrophobicity, or adhesion[1-3]; however, it remains a challenge to achieve a combination of these enhanced properties in a single polymer network. In analogy with alloying in metals, one strategy is to use the constituent monomers from two different polymer networks to form a single material with the combined desired set of properties. The monomer chemistries must be orthogonal to preserve the characteristics of each network rather than creating a single polymer network. Thus, the aim of making an interpenetrating polymer network, or IPN, is to produce a material having the distinct chemical makeup and connectivity of each network by interweaving the two networks together.

IPNs consist of two or more topologically locked polymer networks and vary in degrees of phase separation[2, 4]. IPN applications include light weight restorative and protective structural materials, sound proofing materials, anion exchange membranes[5, 6], mechanically integrous electrical actuators[7], high speed gas sensors[8], tissue scaffolds, and underwater adhesives.[9] All these high performing hybrid materials benefit from some amount of the phase separation and some amount of network interpenetration, the amount of which that is beneficial depends on the application. The enhancement of the modulus, for example, is obtained by network interpenetration, where the densification of chains by complete entanglement increases the resistance to deformation[10]. In contrast, toughness is enhanced by phase separation between the toughening network and the brittle network so that the high energy absorption property of the tough domain is not disrupted. Additionally, the size of the domains must be sufficient to absorb the mechanical energy to prevent crack formation and propagation[11, 12]. Having control over IPN formation for a given network formulation is directly related to controlling the material properties.

There are two general synthetic strategies for IPN formation: sequential and simultaneous.[2, 4] The sequential approach typically is achieved by swelling of a network with monomers that are subsequently polymerized to form a second intertwined network. The simultaneous approach uses monomers that polymerize via orthogonal reaction pathways enabling the simultaneous formation of two intertwined networks. As the distinct macromolecules grow, phase separation can occur due to the entropy loss associated with polymer connectivity. Simultaneously, phase separation is halted by the formation of crosslinks, which act as topological

[a] Department of Chemical and Biomolecular Engineering, University of Delaware, 150 Academy Street, Newark, DE 19716, USA.
[b] Department of Materials Science and Engineering, University of Delaware, 201 DuPont Hall, Newark, DE 19716, USA

† Footnotes relating to the title and/or authors should appear here.
Electronic Supplementary Information (ESI) available: [details of any supplementary information available should be included here]. See DOI: 10.1039/x0xx00000x

constraints preventing the diffusion of chains that would otherwise lead to phase separation. By manipulating IPN formation, the degree of phase separation between the networks and therefore the final properties of the material can be controlled.[13, 14]

Click chemistry provides a facile route for sequential IPN formation. Click reactions are characterized by high selectivity and high yields, ensuring orthogonal network formation in presence of other functional chemistries. Several click reactions, such as the Cu(I)-catalyzed azide–alkyne cycloaddition (CuAAC) and aza-Michael addition reactions, have been used in the synthesis of IPNs[15-19]. Spatiotemporal control of IPN formation is achieved by triggering the click reactions through a photo-initiation scheme. The polymerization will only begin where the light is irradiated and, consequently, the forming material may be patterned to fit the functional specifics of its intended application.

The CuAAC and methacrylate radical polymerizations can be simultaneously photoinitiated to form IPNs.[18] CuAAC polymer networks are formed from multifunctional azide and alkyne monomers in the presence of Cu(I); however, these monomers are unreactive in the presence of Cu(II). The irradiation of a radical photoinitiator generates a radical species that can reduce Cu(II) to Cu(I), which subsequently catalyzes the azide and alkyne monomer copolymerization. In the presence of methacrylate monomer, the radical species can also initiate methacrylate homopolymerization. By combining multifunctional azide, alkyne, and methacrylate monomers with Cu(II) and a photoinitiator, simultaneous IPN formation can be achieved at room temperature in the absence of solvent, as illustrated in Figure 1.

While the simultaneous photopolymerization of CuAAC and methacrylate monomers is triggered using a single radical-based photoinitiator, the respective polymerizations begin at different times designated as an induction time. The CuAAC polymerization occurs before the methacrylate polymerization, implying that radical initiation and propagation is delayed by the presence of Cu(II), which must be sufficiently reduced for methacrylate polymerization to occur. Importantly, the induction time and polymerization rates are readily varied by changing the light intensity.[18] These differences in polymerization formation of the constituent networks (i.e., the CuAAC and methacrylate-based networks) results in different polymerizing environments and ultimately different material properties. Consequently, the mechanical properties are readily controlled by varying light intensity, rather than changing the resin composition.

The kinetic control over material properties in these IPNs is a direct consequence of the sequence in which the constituent networks gel. The gel point is defined as the conversion where single sample-spanning molecule percolates or spans the volume of the system. Radical-initiated polymerization of dimethacrylates, such as TEGDMA, follows a chain-growth mechanism and typically gels within the first 5% conversion of carbon-carbon double bonds[20]. The formation of a network using diazide and trialkyne monomers via the CuAAC reaction follows a step-growth mechanism and is expected to gel at ~71% conversion, as predicted by the Flory-Stockmayer equation.[21, 22] While the photoinitiation of these two polymerizations can be performed simultaneously, the rates of polymerization have a different dependence on the intensity of light; thus, the control of which network (i.e., the CuAAC- or methacrylate-based network) reaches its gel point conversion is readily selected by changing the intensity, which has a significant impact on the IPN molecular architectures and their associated properties.

ARTICLE

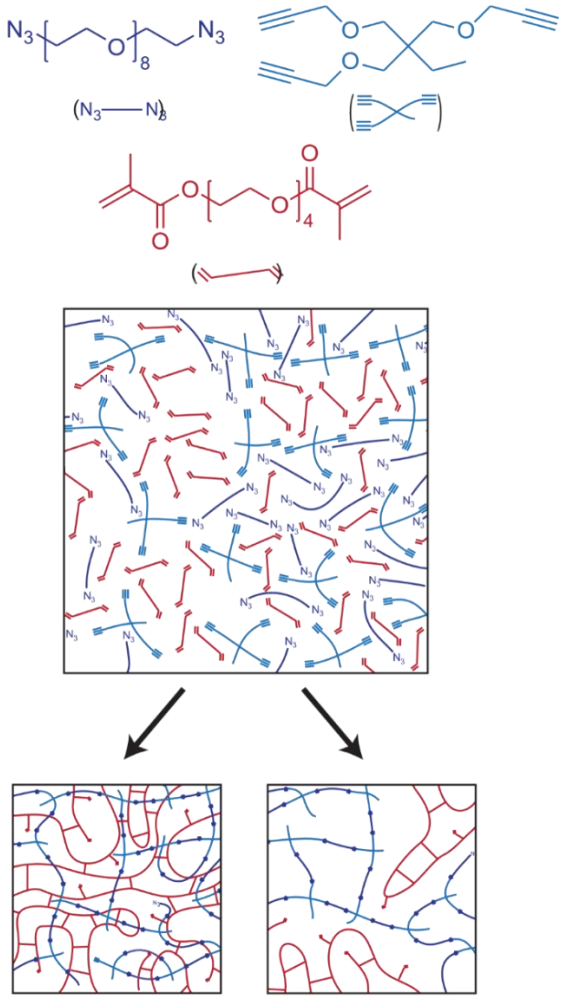

Figure 1. Top) Monomers used in the current study [heptaethylene glycol di(azidoethyl ether) (PEG8 diazide), 1,1,1-tris(propargyl hydroxymethyl)propane (trialkyne), and tetraethylene glycol dimethacrylate (TEGDMA)]. Bottom) Potential network topologies formed assuming a more intertwined, simultaneous mechanism (bottom, left) and a more phase separated, sequential mechanism (bottom, right).

In this study, multifunctional azide and alkyne monomers are mixed with a dimethacrylate monomer to form a photo-CuAAC-methacrylate IPN resin. The CuAAC network is synthesized from a stoichiometric equivalent of PEG8 (eight repeat units of ethylene glycol) diazide and an aliphatic trialkyne crosslinker, and the methacrylate network is synthesized from tetraethylene glycol dimethacrylate (TEGDMA) (Top, Figure 1). By varying light intensity, control over polymerization kinetics, thermomechanical properties and morphology is demonstrated and evaluated.

Experimental

Synthesis of monomers

Poly(ethylene glycol) (PEG400), camphorquinone, and trimethylaniline were purchased from TCI Chemicals. Tetraethylene glycol dimethacrylate, $Cu(II)Cl_2$, and Pentamethyldiethylenetriamine (PMDETA) were purchased from Sigma Aldrich. All other chemicals were purchased from Fisher Scientific.

PEG8 Diazide

The following procedure was modified from Cao et al.[23] To a round bottom flask containing DCM (200 ml), PEG400 (24.6 g, 61.5 mmol) and potassium hydroxide (33 g, 588 mmol) were combined. The round bottom flask was then cooled to 0°C via ice bath. To the reaction mixture, tosyl chloride (24 g, 126 mmol) was added. The reaction mixture was left to stir overnight. The reaction mixture was then washed with water (200 mL x 3) and then extracted with DCM (200 mL x 3). The organic extract was dried with sodium sulfate and then concentrated to yield the ditosylated PEG400 product.

To PEG400 a round bottom flask containing DMSO (100 mL), the ditosylated PEG400 product (12 g, 16.6 mmol) and sodium azide (9.6 g, 148 mmol) were combined. The round bottom flask was heated to 50°C and left to stir overnight. The reaction mixture was then diluted with water (100 mL) and then extracted with ethyl acetate (200 mL x 4). The organic extract was washed with water (100 mL) and then washed with brine (100 mL x 4). The organic extract was dried with sodium sulfate and then concentrated. Chemical compound was confirmed by ^{1}H NMR in $CDCl_3$ (SI Figure 1) ppm: δ 3.38 (4 H, m, CH_2-azide), 3.67 (32 H, m, O-CH_2). Final yield: 5.3 g (11.4 mmol), 69% yield.

Aliphatic Trialkyne – (1-(Prop-2-yn-1-yloxy)-2,2-bis((prop-2-yn-1-yloxy)methyl)butane)

The following procedure was modified from Baranek et al.[24] To a round bottom flask containing DMSO (200 ml), trimethylolpropane (7 g, 52.2 mmol) and potassium hydroxide (28 g, 499 mmol) were combined. The reaction mixture was cooled to 0°C in an ice bath. To the reaction mixture, propargyl bromide, 80 wt.% in toluene (20 mL, 184 mmol) was added dropwise. The reaction mixture was allowed to warm up to room temperature and left to stir overnight. The reaction mixture was then diluted with water (1000 mL) and extracted with diethyl ether (500 mL x 3). The organic extract was concentrated to a volume of 500 mL, and then washed with water (250 mL x 3) and brine (250 mL x 3). The extract was dried

with sodium sulfate and further purified using column chromatography (1:10 ethyl acetate:hexanes). The aliphatic trialkyne product was confirmed by ^{1}H NMR in $CDCl_3$ (SI Figure 2) ppm: δ 0.88 (3H, t, CH_3), 1.43 (2H, q, CH_2-CH_3), 2.40 (3H, t, alkyne-H), 3.41 (6H, s, CH_2), 4.13 (6H, d, CH_2-alkyne). Final yield: 4 g, 31% yield.

Cu(II)Cl_2/PMDETA

Preligation of the copper catalyst followed a modified procedure from El-Zaatari et al.[25] To a round bottom flask charged with acetonitrile (75 mL), Cu(II)Cl_2 (0.85 g, 6.3 mmol) was added and fully dissolved. To the reaction mixture, PMDETA (1.1 g, 6.3 mmol) in acetonitrile (25 mL) was added dropwise, and then left to stir overnight. The reaction mix was concentrated and recrystallized in cold acetone. The product was washed with diethyl ether and dried by evaporation.

IPN Resin Formulation

In a typical formulation, PEG diazide and trialkyne monomers were added to a glass vial at a 1:1 azide:alkyne stoichiometry. Into the mixture of CuAAC monomers, 0.8 wt.% (of CuAAC monomers) of Cu(II)Cl2/PMDETA was added. A minimal amount of methanol was added to the vial to help with dissolution of the ligated Cu(II) catalyst into the resin. Subsequently, the methanol was removed via evaporation, confirmed gravimetrically. The resin was transferred into a Flacktek SpeedMixer cup and mixed at 2500 RPM for 5 minutes. TEGDMA was added to the mixing cup to comprise 75, 50, or 25 wt.% of the total monomer in the mixing cup, depending on the IPN CuAAC-methacrylate composition (25 CuAAC-75 TEGDMA, 50 CuAAC- 50 TEGDMA, or 75 CuAAC- 25 TEGDMA wt.%). The photo-initiating system camphorquinone (CQ) and trimethylaniline (TMA) were added at 0.7 and 1.4 wt.% of the total monomer content to the mixing cup. The mixing cup was then inserted into a Flacktek SpeedMixer, and speedmixed at 2500 RPM for five minutes.

Photopolymerization and in-situ FTIR

The resin injected between two glass slides separated by 0.25 mm thickness shim spacers, using binder clips to hold the structure together. The specimen was placed into an in-house built horizontal FTIR stage that enables simultaneous incident irradiation and FTIR monitoring. The irradiation source was an Omnicure mercury lamp equipped with a 470 nm interference filter in line with liquid lightguide having a collimating lens at its end. The light source, wavelength filter, and liquid lightguide were acquired from Excelitas. The light intensity was measured at the sample end with a photometer. A Thermofisher Nicolet iS50 FTIR was used for monitoring the near-IR peak absorbances at 6430-6570 cm^{-1} (corresponding to the C-H overtone stretch of the alkyne functional group) and at 6145-6185 cm^{-1} (corresponding to the C-H overtone stretch of the methacrylate functional group). First five minutes of FTIR scans were carried out in dark.

Dynamic Mechanical Analysis (DMA)

The thermomechanical properties of the IPN films were measured with a TA DMA Q800 in tension. The IPN films were rectangular with the approximate dimensions of 20 mm x 4 mm x 0.25 mm. The DMA method ran as the following: 1) equilibration at -80°C, 2) isothermal hold for 10 minutes, and 3) ramp to 210°C at 3°C/min, with 0.1% oscillatory strain at 1 Hz frequency.

Atomic Force Microscopy (AFM)

All AFM specimens were microtomed with a Leica cryomicrotome prior to imaging. The films were encapsulated into an epoxy-amine resin supplied by Electron Microscopy Sciences. The resin was cured overnight at room temperature, under vacuum. The material was then cryomicrotomed at -80°C with a glass blade. The cut size was gradually reduced from 500 nm to 100 nm. After numerous 100 nm cuts to the surface, the sample was removed from microtoming and taken to the AFM. The AFM phase images were collected in tapping mode on a Veeco Dimension 3100 AFM using 8nm rectangular tips (specifically, Bruker model NCHV-A tips). The images were collected on a 10 µm x 10 µm scale, with the resolution of 512 samples per line for 512 lines. The scan rate was 1 Hz, the amplitude setpoint varied between 340 and 350 mW, and the drive amplitude was set at 150 mV.

Results and Discussion

The separation of the CuAAC and methacrylate polymerizations is controlled by the intensity of the light. The differences in the induction periods are clearly observed in the photopolymerization conversion vs. time profiles shown in Figure 2 (a, b) for the IPN 50-50 (50 wt.% CuAAC monomers - 50 wt.% TEGDMA) resin photoinitiated with 20 mW/cm^2 and 0.2 mW/cm^2 irradiation, respectively. The methacrylate induction period is attributed to the quenching of excited camphorquinone by Cu(II), as discussed in previous studies,[26] and depicted in Figure 3. The observation that CuAAC polymerization begins before methacrylate polymerization indicates a higher reactivity of the photo-generated radicals to reduce Cu(II) than to initiate methacrylate polymerization. Upon the initial generation of Cu(I), the consumption of alkyne occurs via the CuAAC reaction, even before all the radical-inhibiting Cu(II) is converted to Cu(I). Thus, the catalytic behaviour of Cu(I) in the CuAAC reaction results in an increase in the differences between the induction periods of the CuAAC and methacrylate polymerizations at low light intensity.

ARTICLE

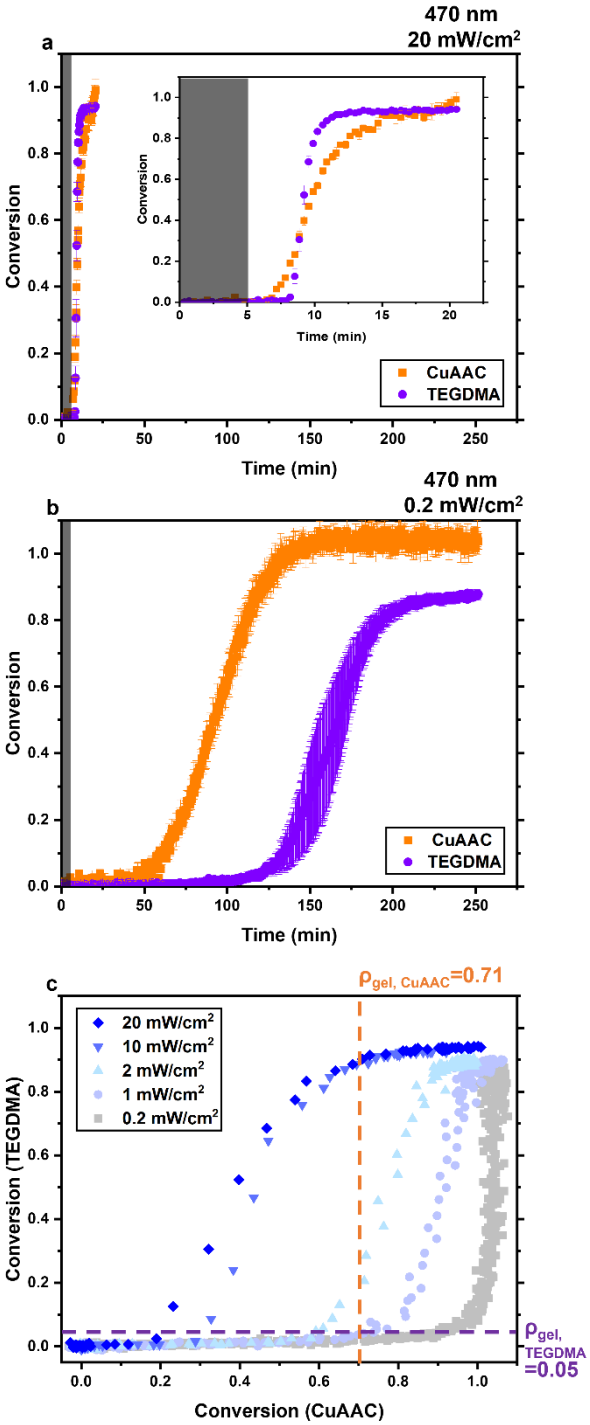

Figure 2. Impact of intensity on IPN kinetics a) Conversion vs. time (min) for IPN 50-50 (50 wt.% PEG8 CuAAC (orange square)- 50 wt.% TEGDMA (purple circle)) under 470 nm irradiation at 20 mW/cm^2 intensity after five initial minutes in dark. b) Conversion vs. Time (min) for IPN 50-50 (CuAAC (orange square)-methacrylate (purple circle)) under 470 nm irradiation at 0.2 mW/cm^2 intensity after five initial minutes in dark. c) Conversion of TEGDMA vs Conversion of CuAAC at the following intensities: 0.2 (gray square), 1 (light violet circle), 2 (light blue upright triangle), 10 (dark blue downward triangle), and 20 mW/cm^2 (blue diamond).

The light intensity not only impacts the induction periods for each polymerization but the overall polymerization kinetics as well. Both polymerizations present auto-acceleration behaviour under moderate to low light intensity irradiation. The triazole product is known to ligate well with both copper species, accelerating the CuAAC reaction kinetics[27]. The effect of this is observed by the auto-acceleration in the CuAAC kinetics for the IPN 50-50 formation at both intensities, 20 and 0.2 mW/cm^2 in Figure 2(a, b). The consumption of alkynes at an accelerating rate with remaining Cu(II) to be reduced at low light intensities allows for a more drastic difference between the induction periods of the CuAAC polymerization and the methacrylate polymerization. The kinetics of the methacrylate polymerization, a free radical chain growth polymerization, in the IPN also exhibits auto-acceleration. As the growing methacrylate polymer chains get larger, the termination rate slows owing to decreased diffusion. The reduction in the termination rate causes the propagation rate to increase as it is dependent on the concentration of actively propagating polymer chains. The phenomenon, termed the Trommsdorf Norrish effect,[28] accelerates the methacrylate polymerization kinetics as observed in Figure 2(a, b).

ARTICLE

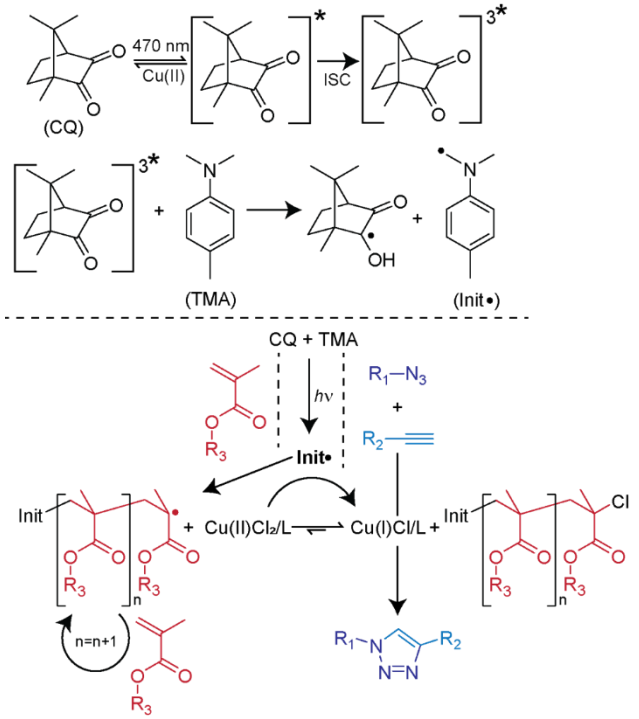

Figure 3. Overall reaction mechanism for simultaneous photo-CuAAC and methacrylate network formation. (top) In the present 470 nm light, camphorquinone (CQ) is excited to its singlet state followed by intersystem crossing (ISC) to a triplet state, which subsequently abstracts a hydrogen from trimethylaniline (TMA) to produce an initiating radical species (Init*). The initiating species can initiate radical polymerization of methacrylate (bottom, left) or reduce copper(II) to copper(I), thus initiating the copper(I)-catalyzed azide–alkyne cycloaddition reaction (CuAAC) (bottom, right). Additionally, the two reactions are coupled through an atom transfer radical polymerization process, consisting of an equilibrium between the growing radical chain and $Cu(II)Cl_2/L$ with the chloride capped chain and Cu(I)Cl/L.

The selection of light intensity affords control over both the time at which each polymerization begins and the rates at which they proceed, thereby affecting the formation of each network within the IPN (Figure 2c). The extent of conversion of a polymerization directly relates to the size and structure of the resulting monomer-oligomer-polymer mixture. The gel-point conversion, or the conversion at which a single molecule percolates the reaction volume, is a critical point in the evolution of network formation. In the formation of an IPN, the network to gel first forms the underlying scaffold of the material, thereby having a significant influence on the formation and structure of the second network. Gelation also typically coincides with the cessation of phase separation.[29, 30] Being able to pick which network gels first, and finely tune where along the formation of both constituent structures gelation occurs is the ultimate advantage of this IPN system.

The compositional ratio of CuAAC to methacrylate monomers within the resin affects network formation; however, within each composition the irradiation intensity has a profound influence over which network forms first. As shown in Figure 4a, the composition has a significant effect on the induction period at the higher intensity (20 mW/cm^2) which is not observed in the lower intensity (20 mW/cm^2). It should be noted that as the CuAAC resin loading is increased, the copper content (0.8 wt.% of the CuAAC portion of the resin) is also increased, which results in greater difference in the induction periods of the polymerizations. In any case, the difference between high and low intensity switches conversion profile between near-simultaneous (20 mW/cm^2) to near-sequential (0.2 mW/cm^2). For all compositions, the methacrylate polymerization reaches the gel-point conversion before the CuAAC polymerization at a photoinitiating intensity of 20 mW/cm^2, whereas the CuAAC polymerization reaches the gel-point conversion before the methacrylate polymerization at an intensity of 0.2 mW/cm^2.

A gradual reduction in intensity from 20 mW/cm^2 to 0.2 mW/cm^2 exhibits a smooth shift in the near simultaneous conversion trajectory (in which the methacrylate polymerization gels first) to the near sequential trajectory (in which the CuAAC polymerization gels first), highlighting the fine tunability of the photo-CuAAC–methacrylate IPN system by only varying the photoinitiation intensity (Figure 2c). While the control over formation kinetics over a range of IPNs have been widely investigated,[31] many of these systems generally focus on the effect of catalyst content and temperature. For those studies that do examine the effects of varying light intensity on photopolymerization of polymer blends,[32] they typically exploit the delay in the onset of Trommsdorff-Norrish effect at low light intensity to the slow reaction kinetics enabling increased phase separation.[32-35] All of these IPN systems do not exhibit photocontrol over which network gels first by only varying the light intensity. This is uniquely achieved by the differences in gelation mechanism (i.e., step versus chain growth mechanism) and the interplay of copper between the two polymerizations. The photo-CuAAC–methacrylate system allows for the choice of which network begins to form first without changing the resin composition.

ARTICLE

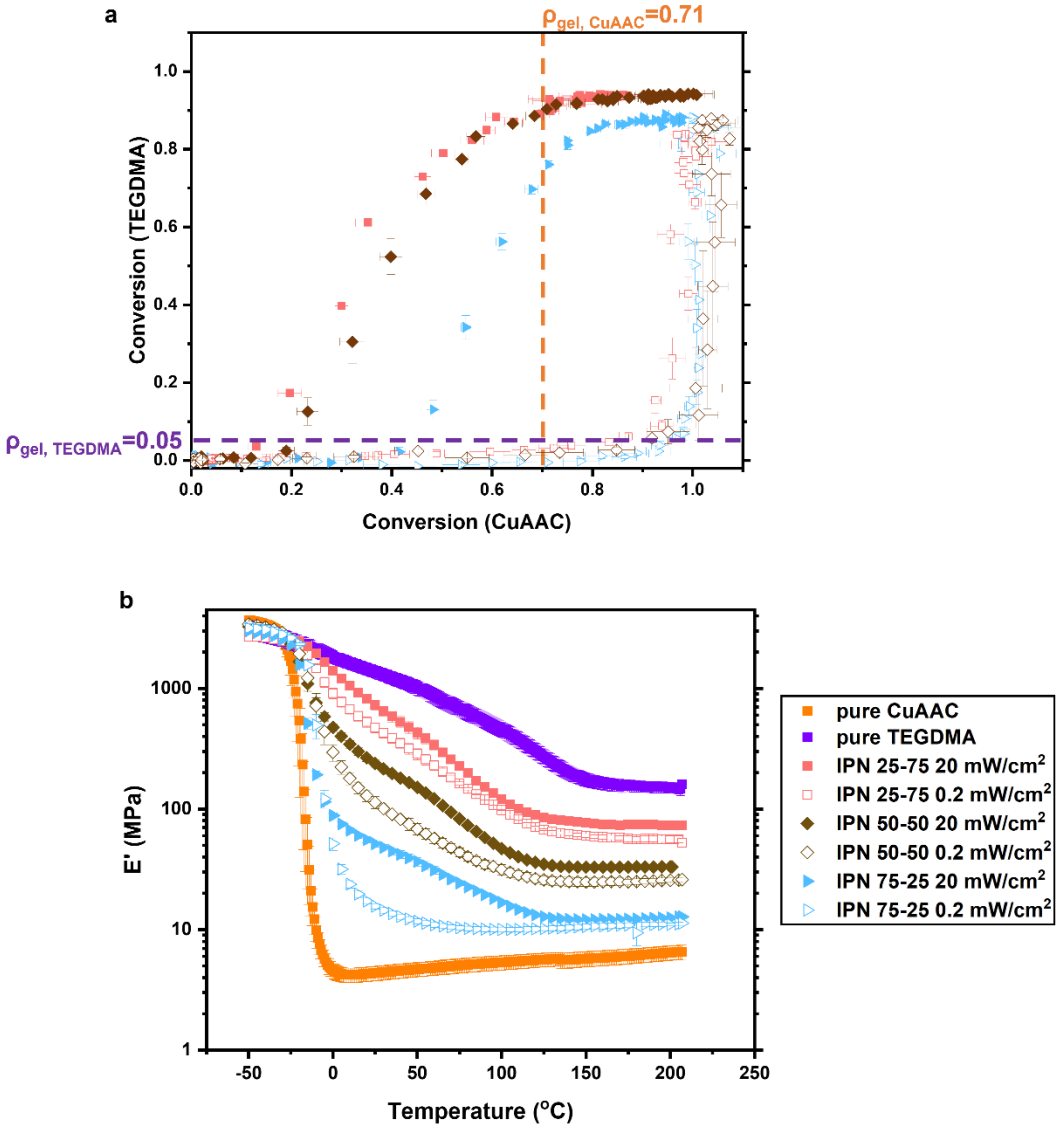

Figure 4. IPN composition and photoinitiation intensity effect on conversion trajectory and linear mechanical properties. a) Conversion of methacrylate vs conversion of CuAAC at compositions of IPN 25-75 (pink square), IPN 50-50 (brown diamond), and IPN 75-25 (light blue triangle) and at intensities of 20 mW/cm² (closed shape) and 0.2 mW/cm² (open shape). b) E' (MPa) vs. Temperature (°C) curves for pure CuAAC network (orange square), pure TEGDMA network (purple circle), and IPNs formed with the following compositions and intensities: 25-75 (pink square), 50-50 (brown diamond), 75-25 (blue triangle) and 20 mW/cm² (closed shape) and 0.2 mW/cm² (open shape)

The thermal behaviour of the IPN elastic modulus is bounded by the elastic moduli of the constituent methacrylate and CuAAC networks (Figure 4b). Dynamic mechanical analysis (DMA) of CuAAC networks in previous studies revealed a homogeneous network with a sharp glass transition,[24, 36] consistent with the thermal behaviour of E' between -20°C and 0°C observed here. The methacrylate network is glassy at room temperature and is a relatively heterogeneous network structure as evident by the broad thermal glassy to rubbery E' transition between -50°C and 150°C; this is also consistent with the literature.[37-39] The 'rubbery' modulus of the methacrylate network and the CuAAC network is ~ 200 MPa and ~10 MPa, respectively, at 200°C (i.e., well above the glass transition). As the rubbery modulus is related to the apparent crosslink density through the theory of rubber elasticity, thus it can be inferred that there are roughly 20x more crosslinks in the methacrylate versus the CuAAC network. Thus, it is not surprising that the compositional differences play a significant role in the magnitude

of the modulus differences in the IPN. As shown in Figure 4b, the thermal response of the elastic modulus transitions from more CuAAC-like to more methacrylate-like from the 75-25, 50-50, and 25-75 IPNs, consistent with the compositional variation.

The photocontrol over which network forms first directly influences the material properties.[2, 4] Generally, low light intensity (0.2 mW/cm^2) polymerizations yielded lower modulus IPNs at room temperature than those synthesized at higher light intensity (20 mW/cm^2). The most notable difference is an apparent second relaxation that is more prominent at higher intensities, which is related to the high-crosslink density methacrylate network gelling before the lower-crosslink density, more homogeneous CuAAC network. The tan(δ) vs temperature profiles shown in Figure 5 more clearly illustrates the differences in the thermal relaxation behaviour. The peak in the tan(δ) is often designated as the glass transition temperature (T_g), whereas the breadth of the peak is related to the distribution of glassy relaxation associated to the heterogeneity of the network. The presence of two distinct tan(δ) peaks in the IPN that are associated with the T_g of the pure networks indicates the presence of separate CuAAC rich and methacrylate-rich regions within the IPN. It should be emphasized that the compositions are identical, thus the differences in properties are solely due to the microphase separation of the individual components and the resultant network topologies.

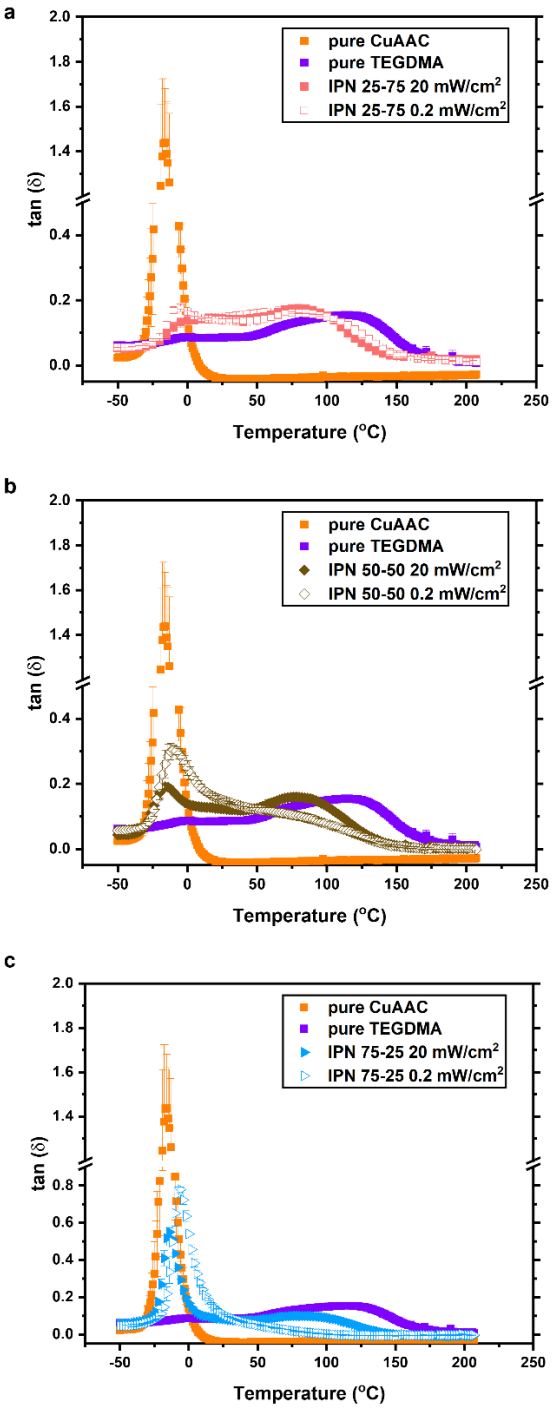

Figure 5. tan(δ) vs. Temperature (°C) curves for a) IPN 25-75, b) IPN 50-50, c) IPN 75-25, with the curves of the pure CuAAC (orange square) and TEGDMA (purple square) networks in each of the plots for reference.

For the 25-75 IPN (i.e., the TEGDMA dominant resin), there are relatively small differences in phase separation between the two intensities as compared with that for the 50-50 and 75-25 IPNs where phase separation is more prominent at the higher intensity 20 mW/cm^2 (Figure 5). At low intensities the CuAAC, step-growth network gels first, suggesting the formation of a uniform network scaffold that suppresses phase separation. The 75-25 IPN resin (i.e., the CuAAC monomer dominant resin)

cured at low intensity (Figure 5c) exhibits is a single peak in the tan(δ).

Phase-contrast imaging in tapping mode atomic force microscopy (AFM) was conducted on the IPN 50-50 films synthesized at 20 and 0.2 mW/cm^2 (Figure 6). The darker, blue/purple phases (larger phase angle) represent softer domains whereas lighter, yellow phases (smaller phase angle) represent harder domains. The significant differences between the two phase images are the discrete/diffuseness of the distinct colours. In the phase image for 20 mW/cm^2, the colours are more discrete, signifying the richness of the hard and soft domains and the overall phase heterogeneity of the material. In the phase image for 0.2 mW/cm^2, the colours are more diffuse, signifying better interpenetration between the hard and soft domains and the overall phase homogeneity of the material. The phase angle distributions indicate that the distribution for 20 mW/cm^2 is broad as compared with the distribution for the 0.2 mW/cm^2. The phase angle distributions correspond well to the thermomechanical data well in that the 20 mW/cm^2 presents more heterogeneous behaviour and the 0.2 mW/cm^2 presents more homogeneous behaviour, both indicating greater interpenetration in 0.2 mW/cm^2 than in 20 mW/cm^2.

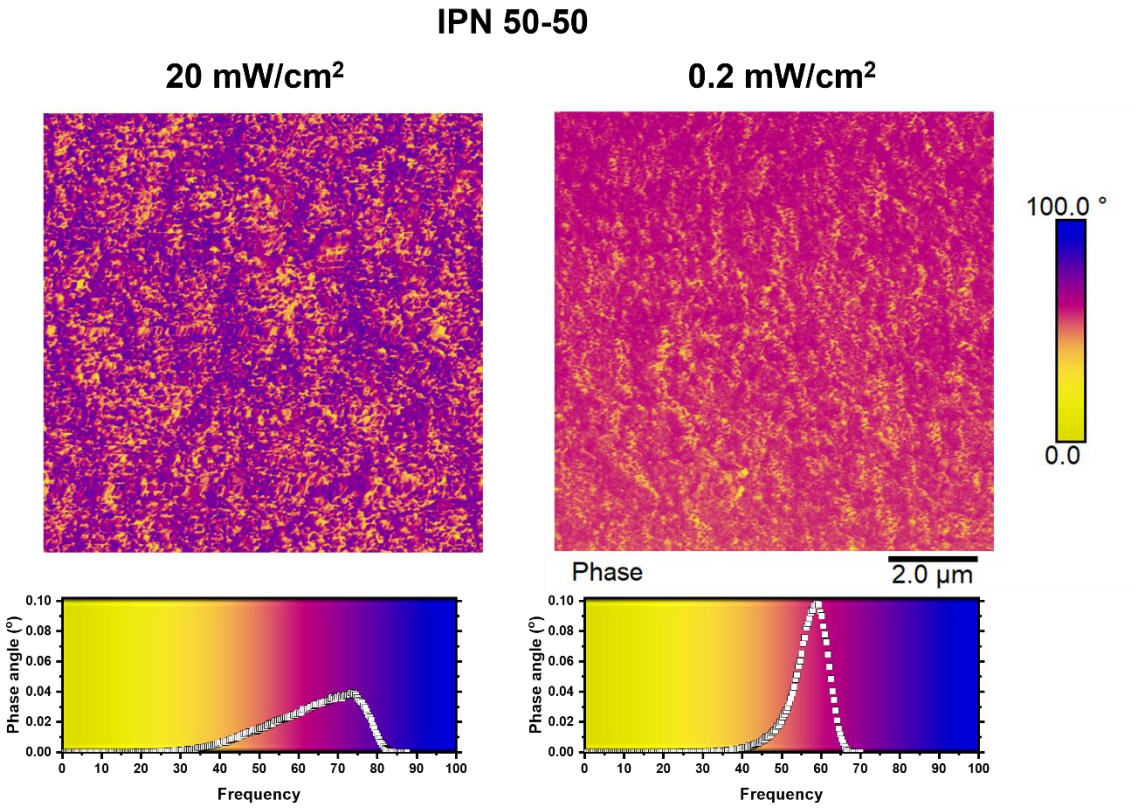

Figure 6. Atomic force phase-contrast micrographs in tapping mode with the corresponding phase angle distributions below. (Top left) Phase image and (Bottom left) phase angle distribution for IPN 50-50 synthesized at 20 mW/cm^2, (Top right) Phase image and (Bottom right) phase angle distribution for IPN 50-50 synthesized at 0.2 mW/cm^2 (all images are 10 µm x 10 µm).

From both morphology and thermomechanical data, the phase integration between the two networks increases with lower light intensity. This observation may seem contrary to expectations as higher rates of crosslinking are expected arrest phase separation and exhibit more interpenetration or phase integration;[32, 40, 41] however, in this system the intensity is directly related to which system gels first. At higher rates of crosslinking, the TEGDMA gels first and may not interpenetrate as well since dimethacrylate monomers tend to form densely entangled regions called microgels that leads to spatial heterogeneity.[42] At lower rates of crosslinking, where the CuAAC phase polymerizes first, providing a more uniform network scaffold in which the methacrylate network must polymerize around. Previous work has shown that if a methacrylate or acrylate network is polymerized further into the conversion of a polyurethane network, a step growth network analogous to the CuAAC network, then a higher degree of interpenetration and a lower degree of phase separation occurs.[13, 43]

Conclusions

Varying the light intensity between 0.2 and 20 mW/cm^2 changes the IPN formation from a simultaneous to sequential mechanism. At the higher intensity of light, the methacrylate polymerization gels before the CuAAC network. At lower intensity of light, the reverse occurs with the CuAAC polymerization gelling before the methacrylate network. The distinct light intensities and corresponding conversions yield materials with different thermomechanical properties and morphologies. At higher light intensities, a greater degree of phase separation between the networks is observed per

thermomechanical data and AFM phase image data. The tan(δ) vs. T (°C) profiles indicate greater differences between the glass transition temperatures of the network dominant phases when polymerized at higher intensities of light than at lower intensities of light. The phase images supplement the thermomechanical observations suggesting more diffuse and smaller phase domains for IPNs polymerized at the lower light intensities, allowing for the inference that a greater degree of interpenetration occurs at lower light intensities. The extent to which the different light intensities and corresponding network formation leads to different material properties is affected by the monomer compositions of the IPN resin. As the CuAAC monomer composition is increased, the distinction between IPNs formed at 20 and 0.2 mW/cm^2 increases. The contrasts are observed in the tan(δ) vs. T(°C) profiles. The common expectation for the synthesis of IPNs is that higher rates of crosslinking leads to less phase separation (i.e., more network interpenetration). This expectation relies on the idea that the topological constraints formed by the crosslinks will impede phase separation and has been confirmed in previous studies; however, this is likely not the case when the first network formed is from monomers prone to microgel formation. In the system presented in this study, the higher the light intensity used for photopolymerization (and therefore the greater the rate of crosslinking) the higher the degree of phase separation that is observed between the constituent networks. This study offers new insights into how IPN kinetics can influence phase separation and property formation, and the inherent simplicity of using photocontrol over property selection can lead to new materials with distinct thermomechanical properties and morphologies from the same resin.

Conflicts of interest

There are no conflicts to declare.

Acknowledgements

This research was partially supported through the NSF EPSCoR Grant No. 1757353 and the State of Delaware. In addition, the NMR and synthetic facility at the University of Delaware were supported by the Center for Hybrid, Active, and Responsive Materials (CHARM) and Centers of Biomedical Research Excellence (COBRE) programs through NSF DMR-2011824 and the NIH NIGMS-P20GM104316, respectively. The authors thank the Keck Center for Advanced Microscopy and Microanalysis at the University of Delaware for use of the AFM instrument.

Notes and references

1. Y. Gu, J. Zhao and J. A. Johnson, *Angewandte Chemie International Edition*, 2020, **59**, 5022-5049.
2. L. H. Sperling and V. Mishra, *Polymers for Advanced Technologies*, 1996, **7**, 197-208.
3. M. S. Silverstein, *Polymer*, 2020, **207**.
4. Y. S. Lipatov and T. T. Alekseeva, *Phase-Separated Interpenetrating Polymer Networks*, 2007.
5. N. Anahidzade, M. Dinari, A. Abdolmaleki, K. F. Tadavani and M. Zhiani, *Energy & Fuels*, 2019, **33**, 5749-5760.
6. L. Zeng, Q. He, Y. Liao, S. Kuang, J. Wang, W. Ding, Q. Liao and Z. Wei, *Research*, 2020, **2020**, 1-11.
7. V. Woehling, G. T. M. Nguyen, C. Plesse, S. Cantin, J. D. W. Madden and F. Vidal, *Sensors and Actuators B: Chemical*, 2018, **256**, 294-303.
8. J. Kim, H. Kweon, H. W. Park, P. Go, H. Hwang, J. Lee, S.-J. Choi and D. H. Kim, *ACS Applied Materials & Interfaces*, 2020, **12**, 55107-55115.
9. J. Liu, S. Wang, Q. Shen, L. Kong, G. Huang and J. Wu, *ACS Applied Materials & Interfaces*, 2020, **13**, 1535-1544.
10. D. R. Paul, in *Multicomponent Polymer Materials*, 1985, DOI: 10.1021/ba-1986-0211.ch001, pp. 3-19.
11. S. Wu, *Journal of Applied Polymer Science*, 1988, **35**, 549-561.
12. S. Monemian and L. T. J. Korley, *Macromolecules*, 2015, **48**, 7146-7155.
13. M. J. Allen, H. M. Lien, N. Prine, C. Burns, A. K. Rylski, X. Gu, L. M. Cox, F. Mangolini, B. D. Freeman and Z. A. Page, *Advanced Materials*, 2022, DOI: 10.1002/adma.202210208.
14. E. Hasa, J. P. Scholte, J. L. P. Jessop, J. W. Stansbury and C. A. Guymon, *Macromolecules*, 2019, **52**, 2975-2986.
15. L. Q. Xu, F. Yao, G. D. Fu and E. T. Kang, *Biomacromolecules*, 2010, **11**, 1810-1817.
16. F. Yao, L. Xu, G.-D. Fu and B. Lin, *Macromolecules*, 2010, **43**, 9761-9770.
17. T. Murakami, H. R. Brown and C. J. Hawker, *Journal of Polymer Science Part A: Polymer Chemistry*, 2016, **54**, 1459-1467.
18. A. U. Shete and C. J. Kloxin, *Polymer Chemistry*, 2017, **8**, 3668-3673.
19. M. Retailleau, J. Pierrel, A. Ibrahim, C. Croutxé-Barghorn and X. Allonas, *Polymers for Advanced Technologies*, 2017, **28**, 491-495.
20. C. Walling, *Journal of the American Chemical Society*, 1945, **67**, 441-447.
21. W. H. Stockmayer, *The Journal of Chemical Physics*, 1944, **12**, 125-131.
22. C. J. Kloxin, T. F. Scott and C. N. Bowman, *Macromolecules*, 2009, **42**, 2551-2556.
23. Y. Cao and J. Yang, *Bioconjugate Chemistry*, 2014, **25**, 873-878.
24. A. Baranek, H. B. Song, M. McBride, P. Finnegan and C. N. Bowman, *Macromolecules*, 2016, **49**, 1191-1200.
25. B. M. El-Zaatari, S. M. Cole, D. J. Bischoff and C. J. Kloxin, *Polymer Chemistry*, 2018, **9**, 4772-4780.
26. B. M. El-Zaatari, A. U. Shete, B. J. Adzima and C. J. Kloxin, *Physical Chemistry Chemical Physics*, 2016, **18**, 25504-25511.
27. S. Neumann, M. Biewend, S. Rana and W. H. Binder, *Macromolecular Rapid Communications*, 2019, **41**.
28. W. D. Cook, *Polymer*, 1992, **33**, 600-609.

29. V. Mishra, F. E. Du Prez, E. Gosen, E. J. Goethals and L. H. Sperling, *Journal of Applied Polymer Science*, 1995, **58**, 331-346.
30. W. Oh, J.-S. Bae and J.-W. Park, *Macromolecules*, 2020, DOI: 10.1021/acs.macromol.0c02520.
31. B. Suthar, H. X. Xiao, D. Klempner and K. C. Frisch, *Polymers for Advanced Technologies*, 1996, **7**, 221-233.
32. Q. Tran-Cong-Miyata and H. Nakanishi, *Polymer International*, 2017, **66**, 213-222.
33. Q. Tran-Cong-Miyata, S. Nishigami, T. Ito, S. Komatsu and T. Norisuye, *Nature Materials*, 2004, **3**, 448-451.
34. D.-T. Van-Pham, X.-A. Trinh, H. Nakanishi and Q. Tran-Cong-Miyata, *Advances in Natural Sciences: Nanoscience and Nanotechnology*, 2010, **1**.
35. T. Ozaki, T. Koto, T. V. Nguyen, H. Nakanishi, T. Norisuye and Q. Tran-Cong-Miyata, *Polymer*, 2014, **55**, 1809-1816.
36. A. U. Shete, B. M. El-Zaatari, J. M. French and C. J. Kloxin, *Chemical Communications*, 2016, **52**, 10574-10577.
37. K. S. Anseth, K. J. Anderson and C. N. Bowman, *Macromolecular Chemistry and Physics*, 1996, **197**, 833-848.
38. K. S. Anseth and C. N. Bowman, *Journal of Polymer Science Part B: Polymer Physics*, 1995, **33**, 1769-1780.
39. L. Rey, J. Galy, H. Sautereau, G. P. Simon and W. D. Cook, *Polymer International*, 2004, **53**, 557-568.
40. Q. Tran Cong, T. Nagaki, O. Yano and T. Soen, *Macromolecules*, 2002, **24**, 1505-1510.
41. Q. Tran Cong, T. Nagaki, T. Nakagawa, O. Yano and T. Soen, *Macromolecules*, 2002, **22**, 2720-2723.
42. H. Galina, K. Dušek, Z. Tuzar, M. Bohdanecky and J. Štokr, *European Polymer Journal*, 1980, **16**, 1043-1046.
43. J.-M. Widmaier, A. Nilly, J.-M. Chenal and A. Mathis, *Polymer*, 2005, **46**, 3318-3322.